STUDY OF LOWER EMITTANCE LATTICES FOR SPEAR3

Xiaobiao Huang[*], Yuri Nosochkov, James A. Safranek, Lanfa Wang
SLAC, Menlo Park, CA 94025, USA

Abstract

We study paths to significantly reduce the emittance of the SPEAR3 storage ring. Lattice possibilities are explored with the GLASS technique. New lattices are designed and optimized for practical dynamic aperture and beam lifetime. Various techniques are employed to optimize the nonlinear dynamics, including the Elegant-based genetic algorithm. Experimental studies are also carried out on the ring to validate the lattice design.

INTRODUCTION

The SPEAR3 storage ring is a third generation light source [1] which has a racetrack layout with a circumference of 234.1 m. The requirement to maintain the photon beamline positions put a significant constraint on the lattice design. Consequently the emittance of SPEAR3 is not on par with some of the recently-built third generation light sources. The present operational lattice has an emittance of 10 nm. For the photon beam brightness of SSRL to remain competitive among the new or upgraded ring-based light sources, it is necessary to significantly reduce the emittance of SPEAR3. In this paper we report our ongoing effort to develop a lower emittance solution for SSRL.

We first show the potential of the SPEAR3 lattice with results of the standard cell study using the GLASS technique [2]. This is followed by a discussion of the design strategy for full-ring linear lattices. Several lattice options are compared. We then show the methods and results for dynamic aperture optimization. Experiments were also conducted on the SPEAR3 ring to implement the lattice and to measure the key lattice parameters.

GLASS FOR A STANDARD CELL

The ring consists of 14 standard cells and 4 matching cells. Both types of cells are double-bend-achromat (DBA) cells. The bending magnets in the matching cells are 25% shorter. The potential of emittance reduction for the ring is mainly determined by the DBA cells. We have studied all possibilities of the SPEAR3 standard DBA cell with a global search of stable solutions [2]. There are three quadrupoles families in the DBA cell, two focusing magnets (QF) and two defocusing magnets (QD) at the ends and a central quadrupole (QFC). We varied the gradients of all three quadrupole families between -2 m^{-2} and 2 m^{-2} with 200 steps and sorted all stable solutions by emittances and optics functions. The color coding of Figure 1 shows the emittance of the cell for all solutions with horizontal
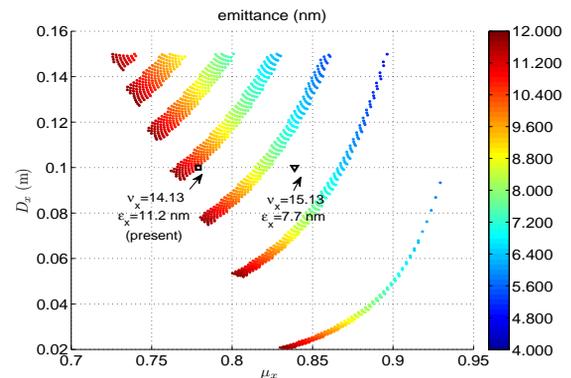
Figure 1: Emittances of stable solutions after a reasonable filter is applied. Each stripe corresponds to a particular value of QFC gradient.

beta below 20 m, vertical beta below 10 m and emittance below 12 nm as a function of horizontal phase advance $\mu_x = \psi_x/2\pi$ and the dispersion function in a straight section. Also indicated in the figure are the standard cells of the present operational lattice and a new lattice that has been tested in experiments. It is seen that the way to reduce emittance is to increase phase advance in the cell or to increase dispersion leak to the straight sections.

Figure 1 shows that there exist cells with emittance below 5 nm. However, there are constraints in the ring design and other requirements for the X-ray source points which could limit the minimum achievable emittance. For example, the matching cells also contribute to the emittance; the overall tunes need to be properly chosen to avoid resistive wall instability and to increase dynamic aperture; the beta functions and dispersion at the source points need to be controlled.

LATTICE DESIGN AND DYNAMIC APERTURE OPTIMIZATION

Linear Lattice Design

Since increasing dispersion leak causes the momentum spread term in the effective emittance at the source point to grow, which partially cancels the emittance reduction, we have focused on the approach of increasing horizontal phase advance in the ring design. The present horizontal tune is 14.13, with a contribution of $\mu = 0.78$ from a standard cell and a dispersion leak of 0.1 m at the insertion devices. By increasing the horizontal tune to 15.13 while keeping the vertical tune at 6.22, we reached a lattice with a bare lattice emittance of 7.7 nm for which the horizontal

02 Synchrotron Light Sources and FELs
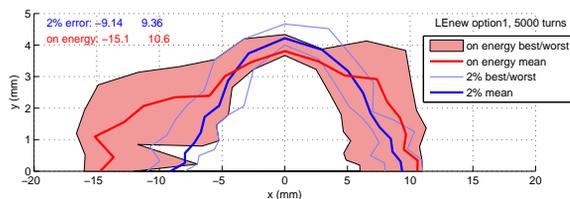
A05 Synchrotron Radiation Facilities

Figure 2: Dynamic aperture of the optimized lattice with working point [15.127, 6.224]. Systematic and random field errors and insertion device non-linearity are included. Beta beating of 1% rms and x/y coupling of 1% are created in all 15 random seeds.
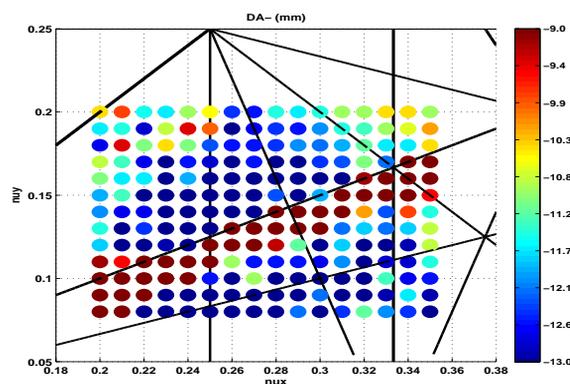

Figure 3: Dynamic aperture of matched lattices on a tune grid.

phase advance per standard cell is $\mu = 0.839$. Considering insertion device damping, the emittance is 6.8 nm, or a 30% reduction from the present value. This lattice was later optimized through a tune scan that varied tunes and phase advances in matching cells for better dynamic aperture. The dynamic aperture of the new lattice (lattice 1 in Table 1) from 15 random seeds is shown in Figure 2.

Tune scans were performed in higher horizontal tune region to search for lower emittance lattices. At each tune point a matched lattice is found using the code MAD8 [3]. Figure 3 shows the dynamic apertures of lattices on a grid with horizontal tune between 15.20 and 15.35. A lattice with a working point of [15.31, 6.10] is chosen as an option (lattice 2 in Table 1).

To further reduce emittance, it is necessary to increase the horizontal tune even more. However, since the amplitude-dependent tune shifts are positive and large in magnitude, the half-integer resonance becomes a barrier that limits the dynamic aperture. When the betatron tunes are above the half integer (e.g., between 15.5 and 16.0), a beam at high current is likely to suffer from resistive wall instability. Nonetheless, we did tune scans in the region with the horizontal tune above 15.5. We searched for lattices with ν_x close to 15.5 so to minimize the resistive wall instability effect. However, the dynamic apertures of these lattices are limited by the $3\nu_x = 2$ resonance. An option

02 Synchrotron Light Sources and FELs

A05 Synchrotron Radiation Facilities

with $\nu_x = 15.54$ is chosen in this region for comparison.

Lattices with horizontal tune above 16 were also considered. These lattices have poor dynamic apertures due to large amplitude-dependent tune shifts. They also have large horizontal beta function at the insertion devices.

Table 1 lists key parameters for some lattices we have considered in comparison to the operational lattice. The amplitude-dependent tune shifts of the new lattices are correlated with the horizontal tune increase and are much larger than the present lattice, which severely limit the dynamic aperture.

Table 1: Comparison of Lattice Options. Dynamic aperture is given at the septum on the inner side.

Parameter	nominal	lat 1	lat 2	lat 3	lat 4
ν_x	14.13	15.127	15.31	15.54	16.13
ν_y	6.22	6.224	6.10	6.17	6.22
μ_x/cell	0.78	0.832	0.844	0.850	0.896
ϵ (nm)	11.2	7.7	7.3	6.9	6.2
ϵ (nm) w/ID	9.6	6.8	6.5	6.1	5.5
$d\nu_x/d\epsilon_x$ m^{-1}	1820	7660	8920	13480	24900
$d\nu_y/d\epsilon_x$ m^{-1}	2120	4980	5590	7810	7880
$d\nu_y/d\epsilon_y$ m^{-1}	2140	4410	4870	6036	4300
DA- (mm)	-17	-15	-13	-7	-7

Dynamic Aperture Optimization

Injection to the ring requires a sufficiently large dynamic aperture, which is limited by nonlinear beam motion. Therefore it is critical to optimize the nonlinear dynamics of the ring. We have mainly adopted a numerical approach, i.e., we vary lattice parameters and calculate the corresponding dynamic aperture by particle tracking to search for an optimum. Genetic algorithms are used in multiple-parameter scans. Two codes have been used for the optimization study: (1) a desktop PC-based matlab script that uses AT [5] and the code NSGA-II [6]; (2) the linux cluster based code Multi-Objective Genetic Algorithm (MOGA) [7].

The parameters (or "knobs") to vary include the tunes, phase advances in matching cells, and sextupole strengths. Presently SPEAR3 has two sextupole families in standard cells and two in matching cells which are powered in series, respectively. In simulation we have tried to split sextupole families into smaller powered-in-series groups to increase the number of knobs, an approach we learned from the successful MOGA application at APS [7]. Figure 4 shows an example of the MOGA application on the lattice with working point [15.127, 6.224] when 21 sextupole knobs are used. This lattice (lattice 1 in Table 1) itself was found with the matlab code.

We have also tried to add harmonic sextupoles to the ring by converting correctors between the QF and QD magnets to combined-function magnets. We found that the new sextupole family can effectively change the detuning coefficients, but in a way such that the sum of $d\nu_x/d\epsilon_x$ and $d\nu_y/d\epsilon_y$ nearly conserves. Consequently the solutions we
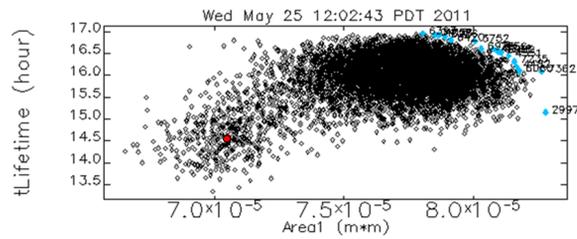
Figure 4: An example of dynamic aperture optimization with MOGA. Red dot represents the starting lattice and the cyan dots represent the resulting best solutions.

found tend to suffer from vertical resonances when magnetic field errors and insertion device nonlinearities are added to the model. Additional octupoles were also tried in simulation.

EXPERIMENTS

We have experimentally implemented the 7.7 nm lattice to SPEAR3. The original lattice (with working point [15.13, 6.22]) had poor injection performance. The injection efficiency was below 0.5% after extensive work on lattice calibration, injection kick bump, sextupole optimization, etc. The new 7.7 nm lattice (lattice 1 in Table 1) had much better performance, with an injection rate over 40% after the linear lattice is calibrated (the injection rate is about 90% for the nominal lattice). A 2-dimensional scan for the sextupoles in the matching cells was carried out, with the sextupoles in standard cells varied accordingly for chromaticity correction. We also performed an experimental tune scan. Results of both scans are shown in Figure 5.

The beam lifetime was measured to be 1.8 hrs with 60 mA stored in 10 bunches while the rf gap voltage was 2.4 MV and the vertical emittance reduced to 4 pm. We varied the rf gap voltage and found that the momentum aperture was not limited by transverse motion for a 2.4 MV gap voltage (or 1.9% momentum aperture).

SUMMARY

Progress has been made for the ongoing SSRL emittance reduction study. We have explored the lattice potentials and studied a few options. It was found that the horizontal tune has to increase to reduce emittance. However, the increase of ν_x is accompanied by a gigantic change of amplitude-dependent tune shifts which cause significant difficulty in assuring sufficient dynamic aperture. Lattices with $\nu_x > 16$ are extremely hard to work with because of large detuning coefficients. Lattices with $15.5 < \nu_x < 16$ suffer from resistive wall instability and dynamic aperture limitation. It appears the promising tune regions are around $\nu_x \approx 15.1$ or 15.3.

Experiments have been carried out on the SPEAR3 ring to verify the new lattices and to understand the require-
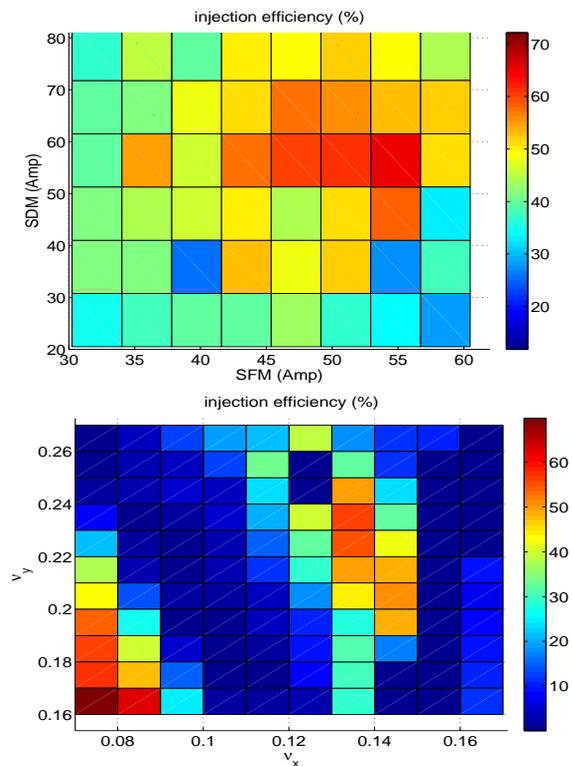
Figure 5: Injection efficiency as the sextupole families SFM/SDM (left) or working point (right) are scanned. Note there was around 10% beta beat in the lattice, resulting higher injection efficiency than the calibrated lattice.

ments for successful operations of these lattices. There is a lattice that had 40% injection efficiency and reasonable lifetime.

We have set up the tools to optimize dynamic aperture using genetic algorithms [6, 7]. There have been some exploration of the tune and sextupole knobs with these tools. But more work is needed to obtain operational lattices.

ACKNOWLEDGMENTS

We thank Michael Borland of APS for helping us set up his ring analysis tool and the MOGA code and for the many useful discussions [4].

REFERENCES

[1] R. Hettel et al., Proceedings of PAC'03, Portland (2003).

[2] D. Robin, W. Wan, TUPMN117, PAC 2007.

[3] H. Grote, F. Iselin, The MAD Program User manual, CERN/SL/90-13, 1996.

[4] M. Borland, APS Report No. LS-287 (2000).

[5] A. Terebilo, Proceedings of PAC'01, Chicago (2001)

[6] K. Deb, IEEE Trans. on Evolutionary Computation, vol 6, no 2, (April 2002).

[7] M. Borland, et al., TH6PFP062, PAC 2009, Vancouver, BC, Canada.